IIETA International Information and Engineering Technology Association
Advancing the World of Information and Engineering

Journal Européen des Systèmes Automatisés
Vol. 58, No. 12, December, 2025, pp. 2635-2645
Journal homepage: http://iieta.org/journals/jesa

Ensuring MPPT Operability in BLDC Solar Pumping Systems: The Critical Role of PV Array Voltage Configuration – An Experimental Study

Noureddine Benbaha[1*], Abdelhak Bouchakour[1], Hachemi Ammar[1], Seif Eddine Boukebbous[2]

[1] Unité de Recherche Appliquée en Energies Renouvelables, Centre de Développement des Energies Renouvelables, Ghardaïa 47133, Algeria
[2] Departement Electrotechnique, Université Frères Mentouri - Constantine 1, Constantine 25017, Algeria

Corresponding Author Email: n.benbaha@cder.dz

https://doi.org/10.18280/jesa.581217

Received: 5 November 2025
Revised: 5 December 2025
Accepted: 12 December 2025
Available online: 31 December 2025

Keywords:
brushless DC motor, photovoltaic water pumping system, MPPT, DC voltage optimization, off-grid solar energy, Saharan climatic conditions

ABSTRACT

This study presents an experimental assessment of the influence of photovoltaic (PV) array voltage configuration on the performance of a 2.2 kW brushless DC (BLDC) solar water pumping system operating under real Saharan climatic conditions in Ghardaia, Algeria. Two PV array topologies, 8S × 1P (245.6 V) and 4S × 2P (122.8 V), were evaluated at three total manometric heads (1 m, 15 m, and 25 m) using a commercial Jntech inverter featuring a maximum power point tracking (MPPT) operating window of 200–400 V. The 8S × 1P configuration consistently maintained the PV voltage above the 200 V threshold, enabling uninterrupted MPPT functionality and achieving system efficiencies of 39–45% along with daily water yields of 30–60 m³. Conversely, the 4S × 2P configuration operated mainly below 200 V (110–135 V), which disabled the MPPT algorithm and forced operation in a fixed-duty-cycle bypass mode, resulting in markedly reduced system efficiencies (8–14%) and water production losses of 60–85%. These findings demonstrate that PV array voltage adequacy rather than array power rating alone is the key determinant of reliable and efficient solar pumping system performance. The results provide practical design guidance for off-grid pumping applications in arid and high-irradiance environments.

1. INTRODUCTION

Due to rapid population growth and the escalating impacts of climate change, conventional energy resources are being depleted at an accelerating rate. This trend has driven a global transition toward renewable energy technologies [1]. Among these, photovoltaic (PV) systems constitute a key component of sustainable energy solutions and are widely deployed in both grid-connected and stand-alone configurations [2]. Through the photovoltaic effect, PV systems convert incident solar radiation directly into direct current (DC) electricity. However, their performance is highly sensitive to environmental factors—particularly temperature, solar irradiance, and cloud cover—which can significantly influence power output [3]. To enable consistent benchmarking, PV module performance is typically evaluated under Standard Test Conditions (STC), defined as an irradiance of 1000 W/m², a cell temperature of 25°C, and an air mass of 1.5.

Individual PV cells may be interconnected in series or parallel to meet specific voltage and current requirements. Series configurations increase the output voltage, whereas parallel configurations enhance the current capacity. A maximum power point tracking (MPPT) controller is then employed to dynamically adjust the electrical load, thereby maximizing energy extraction under varying climatic conditions [4]. This ensures that the array operates at its optimal voltage point. At the device level, a typical PV cell is represented electrically by an equivalent circuit comprising a current source (modeling the generated photocurrent), a diode (representing the p–n junction), a series resistance (accounting for internal ohmic losses), and a shunt resistance (representing leakage currents) [5]. The external load is connected across the cell terminals, and the system's operating point is determined by the intersection of the load's I–V characteristic with the I–V curve of the PV cell.

Owing to their high efficiency, low maintenance requirements, operational simplicity, and compact form factor, brushless DC (BLDC) motors used in solar photovoltaic (SPV) water pumping systems have attracted substantial scientific and industrial attention [6, 7]. However, the intermittent nature of solar irradiance poses a fundamental challenge: water pumping is often disrupted due to the variability and unpredictability of power generation in SPV systems. System operation may cease entirely during adverse weather conditions, periods of low irradiance, nighttime, or extended cloud cover. Moreover, when water demand is low or nonexistent, the solar panels and associated components remain underutilized, resulting in suboptimal use of installed resources. To maintain a continuous water supply under such circumstances, auxiliary power sources become necessary. Historically, diesel generators have served as the primary

backup solution, particularly in rural and off-grid regions [8].

Nevertheless, diesel-based backup systems are increasingly regarded as undesirable due to mounting environmental concerns and the global imperative to reduce greenhouse gas emissions. In remote regions, dependence on fossil fuels also introduces substantial energy security and logistical challenges, including the transportation and storage of fuel. As a result, battery energy storage has emerged as a viable alternative for ensuring uninterrupted operation of SPV water pumping systems. A hybrid configuration that integrates low-voltage SPV arrays with battery storage can provide reliable and dispatchable power, thereby improving system dependability and enabling consistent water delivery regardless of solar availability [9].

As global electricity demand continues to rise, energy efficiency has become a critical priority across all sectors. Within this context, BLDC motors offer notable advantages over conventional induction (asynchronous) motors, including higher efficiency, greater power density, improved power factor, and a superior torque-to-inertia ratio [10]. These performance characteristics have facilitated the widespread adoption of BLDC motors in high-performance applications, particularly in solar-powered water pumping systems. Recent studies emphasize the need for cost-effective, robust, and simplified BLDC motor drive architectures that are specifically designed for hybrid, low-voltage SPV-based pumping installations.

To maximize energy extraction from low-voltage SPV arrays, advanced DC–DC power converters are utilized. The Zeta converter, for example, has proven effective in enhancing usable power under fluctuating irradiance conditions [11]. Likewise, positive-output cascade Luo converters—such as the I-Luo topology—offer high voltage gain with low switching losses, making them well-suited for SPV applications that require elevated DC bus voltages [12]. MATLAB/Simulink simulations have demonstrated that both converter topologies substantially improve system performance during steady-state operation as well as under transient pumping conditions [13].

When integrated with a properly engineered power conditioning unit, BLDC motors enable effective MPPT and significantly enhance the overall reliability and efficiency of the pumping system [14]. The synergistic combination of advanced solar technologies, high-efficiency pumps and motors, and intelligent optimization algorithms is expected to provide researchers and engineers with robust tools for the design, control, and performance optimization of next-generation solar-powered water pumping systems [15].

A variety of drive systems can be employed to operate water pumps, with DC motors, alternating current (AC) motors, and BLDC motors representing the most widely adopted configurations [16]. Among these options, BLDC motors have garnered substantial attention due to their superior performance relative to conventional brushed DC and AC induction motors [17]. Their high efficiency, strong starting torque, reduced maintenance requirements (stemming from the absence of brushes), and compact design make them particularly suitable for small-scale pumping units up to 5.0 kW. Consequently, BLDC motors have become increasingly prevalent in PV array–driven water pumping systems [18].

One effective strategy for mitigating the torque ripple associated with switching in BLDC drives is the use of a simple pulse-width modulation (PWM) current control technique known as deceleration current control, which is straightforward to implement and effective in smoothing the motor response [19]. More advanced control strategies, including field-oriented control (FOC) and sensorless commutation, have also been investigated to further enhance performance in solar water pumping applications [20].

However, because PV cells generate electricity only in the presence of solar irradiance, standalone PV systems require an auxiliary energy storage mechanism to ensure continuous power availability during nighttime or under adverse weather conditions [21]. Among the various energy storage technologies—such as supercapacitors, flywheels, and hydrogen-based systems—electrochemical batteries remain the most widely adopted in off-grid solar PV installations due to their technological maturity, scalability, and cost-effectiveness [22]. Lead–acid batteries, in particular, continue to dominate in developing regions and rural applications because of their low cost, broad availability, and compatibility with low-voltage PV architectures [23], although lithium-ion batteries are increasingly gaining traction owing to their higher energy density and longer cycle life [24].

To maximize energy extraction from the PV array under varying irradiance and temperature conditions, MPPT algorithms are indispensable. Conventional approaches such as Perturb and Observe (P&O) and Incremental Conductance (IncCond) remain widely adopted due to their simplicity and ease of implementation [25]. However, these techniques often exhibit oscillatory behavior around the maximum power point (MPP) and respond sluggishly to rapid changes in environmental conditions. In contrast, intelligent MPPT methods—including fuzzy logic control [26], neural networks [27], and other adaptive algorithms—have demonstrated superior tracking precision, faster convergence, and enhanced robustness in solar water pumping applications [28].

Despite the extensive research on BLDC-driven solar pumping systems, few studies have experimentally investigated the critical influence of DC-link voltage levels—relative to inverter input specifications—on overall system efficiency under real-field, off-grid conditions. This gap is particularly pronounced in arid and high-irradiance regions where optimal sizing of PV arrays remains a practical challenge. To address this, the present study experimentally evaluates a 2.2 kW three-phase BLDC motor-based photovoltaic water pumping system powered by a 240 Wp polycrystalline array under actual Saharan climatic conditions in Ghardaia, Algeria, across varying pumping depths. The results demonstrate that peak system efficiency is achieved when the inverter's DC input voltage operates near its upper permissible limit—a finding with direct implications for PV module selection and system design. By translating empirical observations into actionable engineering guidelines, this work contributes to the development of more efficient, reliable, and cost-effective solar water pumping solutions for remote and resource-constrained communities.

Due to rapid population growth and the escalating impacts of climate change, conventional energy resources are being depleted at an accelerating rate. This trend has driven a global transition toward renewable energy technologies [1]. Among these, PV systems constitute a key component of sustainable energy solutions and are widely deployed in both grid-connected and stand-alone configurations [2]. Through the photovoltaic effect, PV systems convert incident solar radiation directly into DC electricity. However, their performance is highly sensitive to environmental factors—particularly temperature, solar irradiance, and cloud cover—

which can significantly influence power output [3]. To enable consistent benchmarking, PV module performance is typically evaluated under STC, defined as an irradiance of 1000 W/m², a cell temperature of 25°C, and an air mass of 1.5.

Individual PV cells may be interconnected in series or parallel to meet specific voltage and current requirements. Series configurations increase the output voltage, whereas parallel configurations enhance the current capacity. A MPPT controller is then employed to dynamically adjust the electrical load, thereby maximizing energy extraction under varying climatic conditions [4]. This ensures that the array operates at its optimal voltage point. At the device level, a typical PV cell is represented electrically by an equivalent circuit comprising a current source (modeling the generated photocurrent), a diode (representing the p–n junction), a series resistance (accounting for internal ohmic losses), and a shunt resistance (representing leakage currents) [5]. The external load is connected across the cell terminals, and the system's operating point is determined by the intersection of the load's I–V characteristic with the I–V curve of the PV cell.

Owing to their high efficiency, low maintenance requirements, operational simplicity, and compact form factor, BLDC motors used in solar photovoltaic (SPV) water pumping systems have attracted substantial scientific and industrial attention [6, 7]. However, the intermittent nature of solar irradiance poses a fundamental challenge: water pumping is often disrupted due to the variability and unpredictability of power generation in SPV systems. System operation may cease entirely during adverse weather conditions, periods of low irradiance, nighttime, or extended cloud cover. Moreover, when water demand is low or nonexistent, the solar panels and associated components remain underutilized, resulting in suboptimal use of installed resources. To maintain a continuous water supply under such circumstances, auxiliary power sources become necessary. Historically, diesel generators have served as the primary backup solution, particularly in rural and off-grid regions [8].

Nevertheless, diesel-based backup systems are increasingly regarded as undesirable due to mounting environmental concerns and the global imperative to reduce greenhouse gas emissions. In remote regions, dependence on fossil fuels also introduces substantial energy security and logistical challenges, including the transportation and storage of fuel. As a result, battery energy storage has emerged as a viable alternative for ensuring uninterrupted operation of SPV water pumping systems. A hybrid configuration that integrates low-voltage SPV arrays with battery storage can provide reliable and dispatchable power, thereby improving system dependability and enabling consistent water delivery regardless of solar availability [9].

As global electricity demand continues to rise, energy efficiency has become a critical priority across all sectors. Within this context, brushless DC (BLDC) motors offer notable advantages over conventional induction (asynchronous) motors, including higher efficiency, greater power density, improved power factor, and a superior torque-to-inertia ratio [10]. These performance characteristics have facilitated the widespread adoption of BLDC motors in high-performance applications, particularly in solar-powered water pumping systems. Recent studies emphasize the need for cost-effective, robust, and simplified BLDC motor drive architectures that are specifically designed for hybrid, low-voltage SPV-based pumping installations.

To maximize energy extraction from low-voltage SPV arrays, advanced DC–DC power converters are utilized. The Zeta converter, for example, has proven effective in enhancing usable power under fluctuating irradiance conditions [11]. Likewise, positive-output cascade Luo converters—such as the I-Luo topology—offer high voltage gain with low switching losses, making them well-suited for SPV applications that require elevated DC bus voltages [12]. MATLAB/Simulink simulations have demonstrated that both converter topologies substantially improve system performance during steady-state operation as well as under transient pumping conditions [13].

When integrated with a properly engineered power conditioning unit, BLDC motors enable effective MPPT and significantly enhance the overall reliability and efficiency of the pumping system [14]. The synergistic combination of advanced solar technologies, high-efficiency pumps and motors, and intelligent optimization algorithms is expected to provide researchers and engineers with robust tools for the design, control, and performance optimization of next-generation solar-powered water pumping systems [15].

A variety of drive systems can be employed to operate water pumps, with DC motors, AC motors, and BLDC motors representing the most widely adopted configurations [16]. Among these options, BLDC motors have garnered substantial attention due to their superior performance relative to conventional brushed DC and AC induction motors [17]. Their high efficiency, strong starting torque, reduced maintenance requirements (stemming from the absence of brushes), and compact design make them particularly suitable for small-scale pumping units up to 5.0 kW. Consequently, BLDC motors have become increasingly prevalent in PV array–driven water pumping systems [18].

One effective strategy for mitigating the torque ripple associated with switching in BLDC drives is the use of a simple pulse-width modulation (PWM) current control technique known as deceleration current control, which is straightforward to implement and effective in smoothing the motor response [19]. More advanced control strategies, including field-oriented control (FOC) and sensorless commutation, have also been investigated to further enhance performance in solar water pumping applications [20].

However, because PV cells generate electricity only in the presence of solar irradiance, standalone PV systems require an auxiliary energy storage mechanism to ensure continuous power availability during nighttime or under adverse weather conditions [21]. Among the various energy storage technologies—such as supercapacitors, flywheels, and hydrogen-based systems—electrochemical batteries remain the most widely adopted in off-grid solar PV installations due to their technological maturity, scalability, and cost-effectiveness [22]. Lead–acid batteries, in particular, continue to dominate in developing regions and rural applications because of their low cost, broad availability, and compatibility with low-voltage PV architectures [23], although lithium-ion batteries are increasingly gaining traction owing to their higher energy density and longer cycle life [24].

To maximize energy extraction from the PV array under varying irradiance and temperature conditions, MPPT algorithms are indispensable. Conventional approaches such as Perturb and Observe (P&O) and Incremental Conductance (IncCond) remain widely adopted due to their simplicity and ease of implementation [25]. However, these techniques often exhibit oscillatory behavior around the maximum power point (MPP) and respond sluggishly to rapid changes in

environmental conditions. In contrast, intelligent MPPT methods—including fuzzy logic control [26], neural networks [27], and other adaptive algorithms—have demonstrated superior tracking precision, faster convergence, and enhanced robustness in solar water pumping applications [28].

Despite the extensive research on BLDC-driven solar pumping systems, few studies have experimentally investigated the critical influence of DC-link voltage levels—relative to inverter input specifications—on overall system efficiency under real-field, off-grid conditions. This gap is particularly pronounced in arid and high-irradiance regions where optimal sizing of PV arrays remains a practical challenge. To address this, the present study experimentally evaluates a 2.2 kW three-phase BLDC motor-based photovoltaic water pumping system powered by a 240 Wp polycrystalline array under actual Saharan climatic conditions in Ghardaia, Algeria, across varying pumping depths. The results demonstrate that peak system efficiency is achieved when the inverter's DC input voltage operates near its upper permissible limit—a finding with direct implications for PV module selection and system design. By translating empirical observations into actionable engineering guidelines, this work contributes to the development of more efficient, reliable, and cost-effective solar water pumping solutions for remote and resource-constrained communities.

2. METHODOLOGY

The main objective of this study is to evaluate the performance of two solar-powered water pumping systems (4S2P and 8S1P) and to investigate their behaviors under challenging semi-arid conditions. To this end, a critical analysis is conducted based on daily performance parameters, such as daily flow rate, power consumption, and system efficiency under various weather conditions.

2.1 Description of the studied area

Ghardaïa is a Saharan city. Its climate is hot semi-arid, with average summer temperatures between 25 and 4°C and relatively mild winters ranging from 6 to 18°C. According to the World Solar Atlas (SOLARGIS), the average annual global horizontal irradiance (GHI) covering the period 1994-2018 reached approximately 5.82 kWh/m²/day and a maximum of approximately 7.45 kWh/m²/day, while the sunshine duration exceeds 3,200 hours per year.

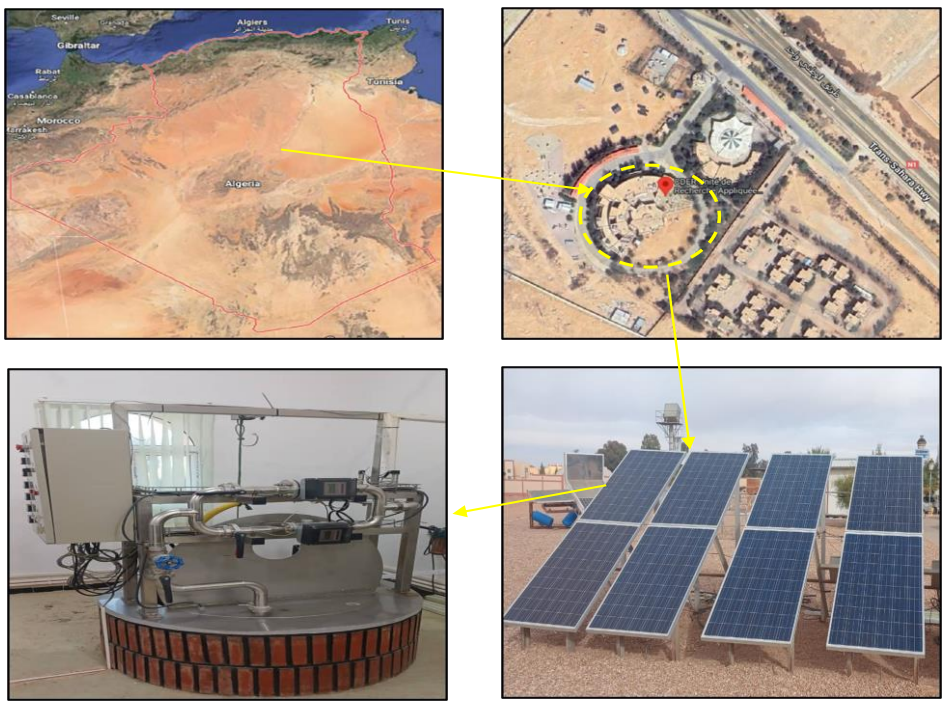

Figure 1. Satellite image of the study area

PV solar pumping systems represent a promising application of PV energy. The city of Ghardaïa offers particularly favorable conditions for the development and testing of this type of technology.

In this context, a 2 kWp system was installed in a demonstration platform dedicated to agricultural renewable energies (located at 3.78° East longitude and 32.38° North latitude). Located within the Ghardaïa Renewable Energy Research Unit (URAER, CDER), this system supplies the electricity for URAER PV pumping test bench in a semi-arid climate, while allowing the evaluation of its performance based on the data collected (Figure 1).

2.2 Experimental system details

The PV generator covers an area of approximately 13 m², consists of eight 250 Wp modules (model: CEM-250P-60). All the PV panels are oriented and inclined at 32° to the south. The DC generated by the PV field is converted into AC using off-grid solar inverter from Jntech (Figure 2). The electrical characteristics of PV generator and the inverter are presented in Table 1.

The overall energy conversion efficiency of a solar water pumping system is defined as the ratio of hydraulic power output to electrical power input from the PV array:

$$\eta_{sys} = \frac{P_{hyd}}{P_{pump}} = \frac{\rho \cdot g \cdot Q \cdot H}{P_{pump}} \quad (1)$$

ρ = density of water = 1000 kg/m³.
g = gravitational acceleration = 9.81 m/s².
Q = water flow rate in m³/s.
H = total manometric head (HMT) in meters.
$P_{pump} = V_{PV} * I_{PV}$.

2.3 Testing procedure

The TDH was regulated by a manual gate valve installed at the pump outlet (Figure 2). The desired pressure setpoints (1 m, 15 m, and 25 m) were verified in real time using an integrated pressure display. Once the required pressure level (the corresponding total dynamic head) was confirmed, the valve was mechanically locked to prevent any unintentional variation during data acquisition. This method ensured a stable and reproducible hydraulic head throughout the testing period.

A complete, autonomous monitoring system, equipped with various sensors, was implemented (Figure 3). It allows for the real-time acquisition of meteorological parameters (ambient/cell temperature and solar radiation) as well as electrical parameters (IPV, PPV, VPV, HMT, water flow rate). This data is essential for analyzing the system's behavior.

Table 1. Detailed experimental setup and instrumentation

Category	Component	Model / Specification	Key Parameters	Accuracy / Notes
PV Array	Module Type	Condor Polycrystalline	250 Wp per module	STC: 1000 W/m², 25°C, AM1.5
	Quantity & Config.	8 modules total	8S×1P: *V*mp = 245.6 V, *I*mp = 8.15 A 4S×2P: *V*mp = 122.8 V, *I*mp = 16.3 A	Total array power: 2000 W
Inverter / MPPT Controller	Model	Jntech 4JDSS11-120-300-2200-A/D	Rated power: 2.2 kW DC input range: 80–420 V MPPT window: 200–400 V	Low-voltage protection activates below 200 V
BLDC Pump	Model	4JDSS11-120-300-2200-A/D	Max. flow: 11 m³/h, Max. head: 120 m, Rated power: 2.2 kW	Performance curve provided in Figure A1.
Sensors	Current	SHUNT-EMB2	Range: 1–500 A, Output: 50/100 mV	±0.1% accuracy, 15 ppm/°C thermal stability
	Voltage	Agilent 34970A (direct measurement)	Input impedance: >10 MΩ	±0.1% of reading
	Flow rate	Inline electromagnetic flowmeter	Range: 0–15 m³/h	±2% of reading
	Pressure	Digital pressure transducer	Range: 0–600 kPa	±1% full scale
	Irradiance	Solar cell–based pyranometer	Range: 0–1200 W/m²	±5% uncertainty
	PV Temperature	PT100 RTD	Range: −50°C to +100°C	±0.5°C
Data Acquisition	System	Agilent 34970A	Channels: 8 analog inputs, Sampling frequency: 0.1 Hz (1 sample / 15 s)	Synchronized real-time clock; data logged to PC

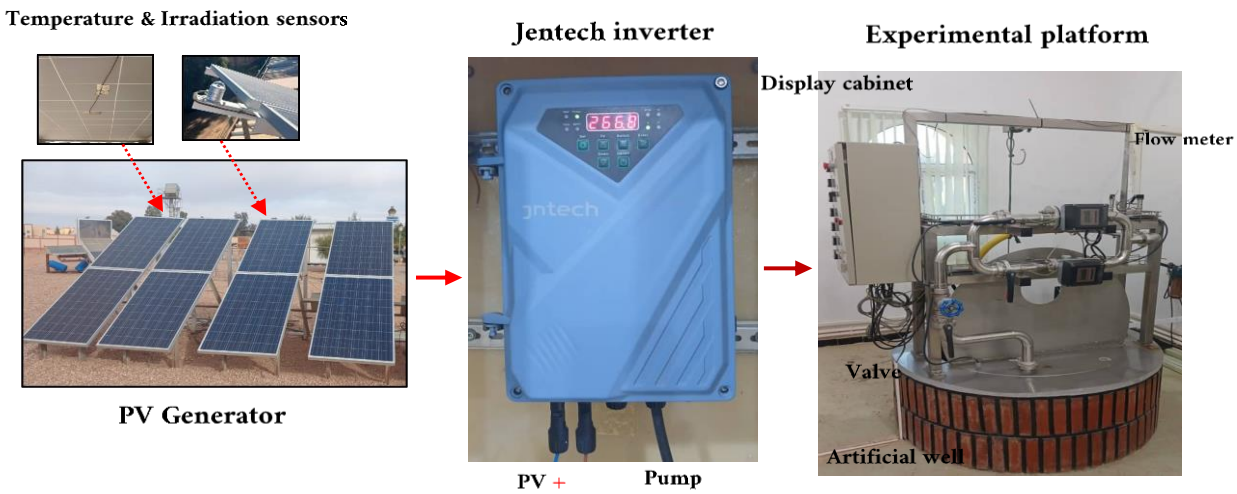

Figure 2. The architecture of the proposed PV pumping system

The data acquisition system includes a pyranometer (solar sensor) installed on the same inclined plane as the PV generator to measure global horizontal solar radiation during the day, two Pt100 temperature sensors for measuring ambient and cell temperatures, and an Agilent 34970A data logger. Meteorological and electrical data are automatically collected every 15 seconds and transferred to a computer via an RS-232 communication link for recording and analysis.

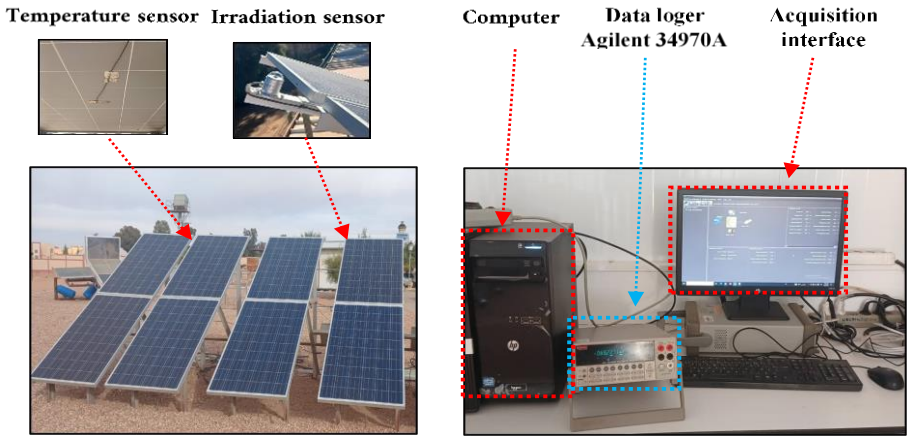

Figure 3. Sensors and data collection instruments

3. RESULTS AND DISCUSSION

The experimental evaluation was conducted using a Jntech 2200 W solar pump (specifications provided in Table A1 and Figure A1). Data were collected on multiple days representing naturally varying environmental conditions, allowing assessment of system performance under realistic fluctuations in solar irradiance and PV electrical output.

3.1 PV generators characteristics

Figures 4-7 illustrate the current–voltage and power–voltage characteristics of the two PV generator configurations described in Table 1. The influence of environmental conditions on electrical performance is clearly evident. Increasing solar irradiance results in higher short-circuit current and enhancement of the maximum power point, reflecting the additional photon flux available for energy conversion. Conversely, elevated cell temperature causes a reduction in open-circuit voltage due to the negative temperature coefficient of the PV modules, which consequently lowers the achievable output power. These trends emphasize the combined sensitivity of PV performance to irradiance and temperature variations under real operating conditions.

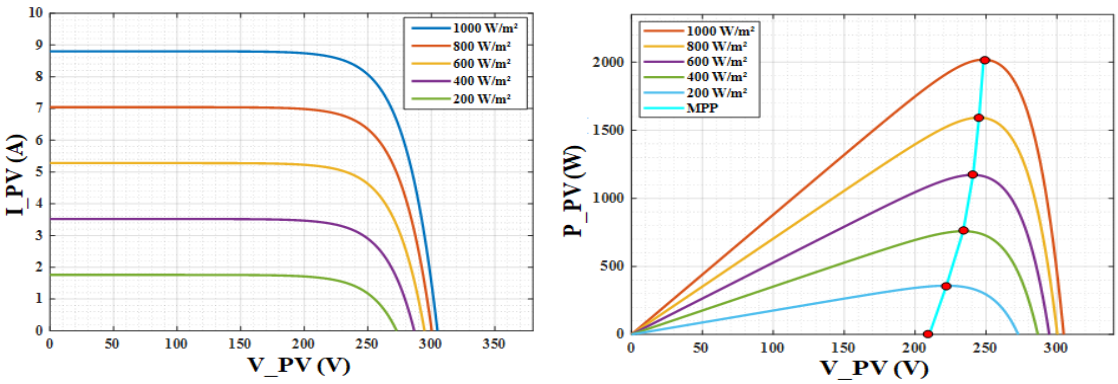

Figure 4. Effect of irradiance variation on the I-V and P-V characteristics for the 8S × 1P

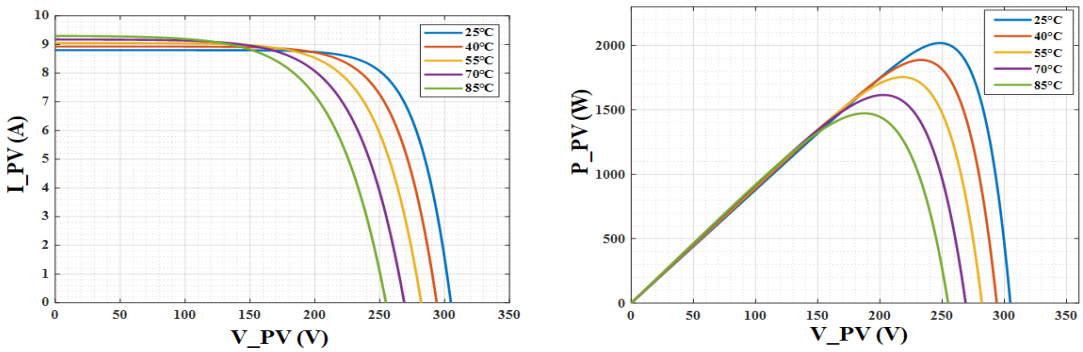

Figure 5. Effect of temperature variation on I-V and P-V characteristics for the 8S × 1P

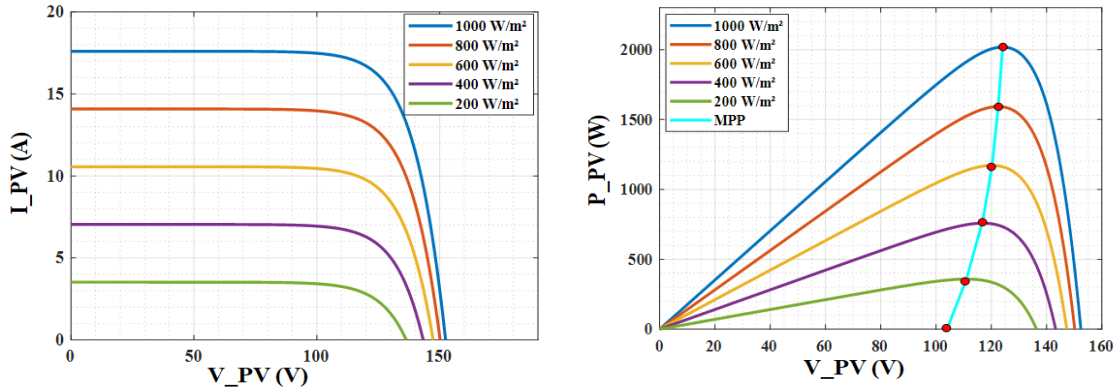

Figure 6. Effect of irradiance variation on the I-V and P-V characteristics for the 4S × 2P

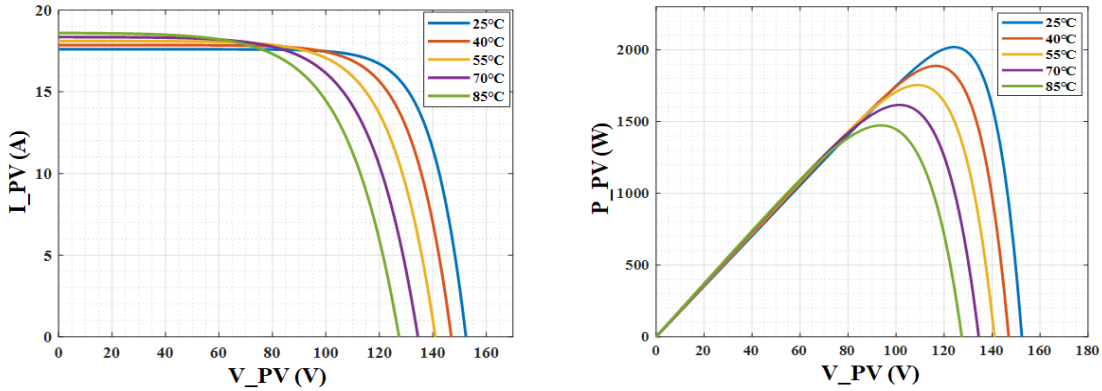

Figure 7. Effect of temperature variation on I-V and P-V characteristics for the 4S × 2P

3.2 Experimental results

Figure 8 shows the daily variation of the voltage for the two configurations (8S1P and 4S2P) as a function of the cell temperature at H = 25 m.

As shown in the figure, when the temperature of the PV cells rises above 50°C, the operating voltage of the PV generator decreases for the two configurations.

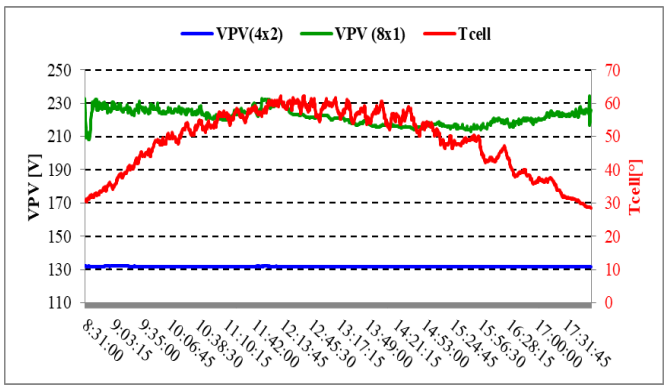

Figure 8. Daily variation of the voltage as a function of the cell temperature

In the 4S2P configuration, the nominal open-circuit string voltage is approximately 122.8 V, which lies below the lower MPPT operating threshold of 200 V. Under such conditions (VPV < 200 V), the controller automatically disables the MPPT algorithm and transitions into a protective fixed-duty bypass mode (≈20%). In this state, the boost converter is unable to dynamically adjust its duty cycle to seek the true maximum power point. Consequently, the system ceases to benefit from increased solar input, leading to persistent underutilization of the PV array's power potential.

By contrast, the 8S1P configuration provides a nominal operating voltage of approximately 245.6 V, which lies comfortably within the required 200–400 V MPPT activation window. This allows the converter to operate continuously and reliably, enabling the converter to draw current close to the module's maximum power point current (Imp) and thereby extract significantly more power throughout the day.

Figure 9 shows the daily variation of the PV generator current for the two configurations (8S1P and 4S2P) as a function of the solar irradiation at H = 25 m.

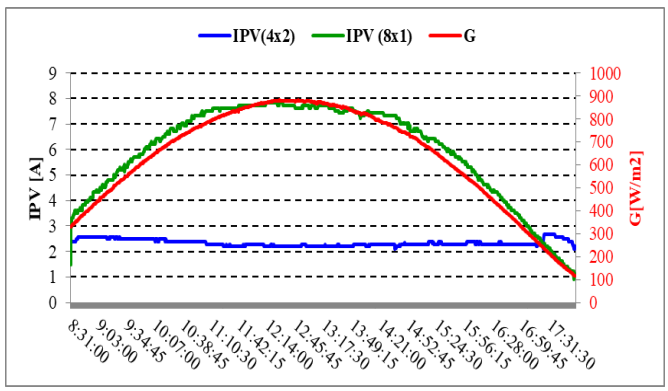

Figure 9. Daily variation of the PV generator current as a function of the solar irradiation

The figure illustrates a clear divergence in PV current behavior between the two array configurations. In the 8S1P

arrangement, the current profile closely follows the diurnal irradiance trend, with IPV rising to approximately 7.8 A near solar noon very close to the theoretical maximum power point current (Imp ≈ 8.15 A). This smooth and symmetric curve confirms that the array is operating near its MPP under most conditions, demonstrating stable and efficient energy extraction facilitated by continuous MPPT engagement.

Conversely, the 4S2P configuration exhibits a nearly constant current of around 2.5 A throughout the day, with negligible response to the increase in irradiance. This flat behavior indicates persistent operation far below the array's potential, directly resulting from the inadequate nominal string voltage (122.8 V), which prevents the MPPT controller from dynamically tracking the MPP.

Figure 10 shows the daily variation of the consumed pump power for the two configurations at H = 25 m. A similar performance gap is evident in the pump power outcomes. For the 8S1P configuration, P_{pump} increases from approximately 700 W during the morning to a midday peak of 1.8 kW, reflecting the system's ability to draw higher current at sufficient operating voltage (220–270 V). In contrast, the 4S2P configuration remains voltage-limited and, consequently, power-limited, with P_{pump} consistently restricted to 300 W over the entire operating period. A brief spike observed near 17:30 appears anomalous and does not indicate any meaningful improvement in performance. Together, these results confirm that the 4S2P configuration operates far below its hydraulic and electrical capability due solely to its inability to sustain MPPT functionality.

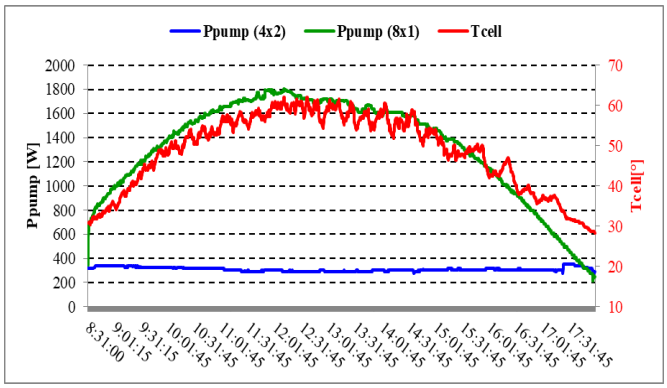

Figure 10. Daily variation of the consumed pump power

Figure 11 shows the daily variation of the flow rate for the two configurations at H = 25 m.

For the 8S1P configuration, the measured flow rate initiates at approximately 3.1 $m^3 \cdot h^{-1}$ in the early morning and increases steadily to a peak of around 7.8 $m^3 \cdot h^{-1}$. Thereafter, it gradually declines with decreasing solar availability, reaching values below 1 $m^3 \cdot h^{-1}$ by late afternoon (≈17:47). This smooth, bell-shaped profile closely follows the irradiance trend and indicates continuous and effective conversion of solar energy into hydraulic output, particularly during midday when MPPT operation is fully maintained.

In contrast, the flow rate remains largely constrained at approximately 1.5 $m^3 \cdot h^{-1}$ over most of the day, showing minimal sensitivity to irradiance fluctuations. A brief spike to approximately 5.5 $m^3 \cdot h^{-1}$ is observed near 17:00; however, this transient deviation is followed by an immediate return to baseline levels and does not reflect a sustained improvement in operating conditions. The predominantly flat flow-rate trajectory confirms that the 4S2P configuration functions far below its hydraulic potential, consistent with the voltage-limited behavior and absence of MPPT engagement described in the previous sections.

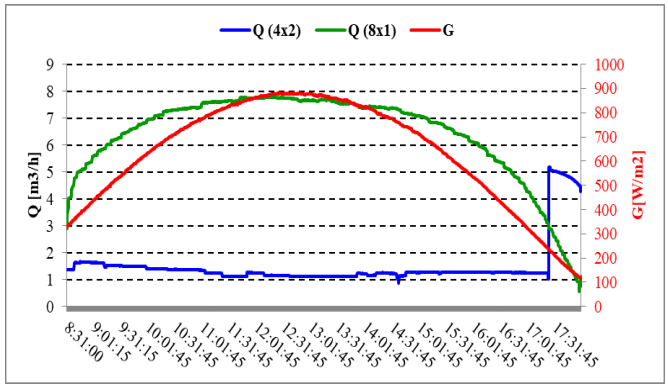

Figure 11. Daily variation of the flow rate

Figures 12 and 13 provide a unified evaluation of system efficiency (η_sys) as a function of PV array operating voltage (VPV) under three total heads (1 m, 15 m, and 25 m). In the 4S2P case (Figure 12), all operating points lie within a narrow low-voltage band (~110–130 V), which corresponds to η_{sys} values of only 8–14% irrespective of head. Although the lowest head (1 m) yields slightly higher efficiency than the highest head (25 m), all curves remain confined to a region well below the inverter's MPPT activation. Thus, the apparent voltage efficiency trend is not indicative of successful power optimization, but instead reflects the inherent limitations of operating in the controller's fixed-duty bypass mode. These results confirm that the 4S2P configuration experiences persistent and unavoidable underperformance due to its inability to achieve the voltage necessary for MPPT engagement.

By contrast, the 8S1P configuration (Figure 13) consistently operates within the inverter's valid MPPT voltage window. In this regime, all three heads achieve markedly higher efficiency, clustered between 40–45%. The slight decrease in efficiency observed as head increases from 1 m to 25 m is fully consistent with the expected rise in hydraulic and mechanical losses at elevated pressure loads, rather than any deficiency in electrical performance. The strong voltage efficiency correlation in this configuration demonstrates continuous and effective MPPT functionality, enabling substantially greater energy transfer from the PV array to the pump. Together, figures establish that PV voltage adequacy, not head variation, is the dominant factor governing system efficiency, reinforcing the critical role of array topology in matching the inverter's operational requirements.

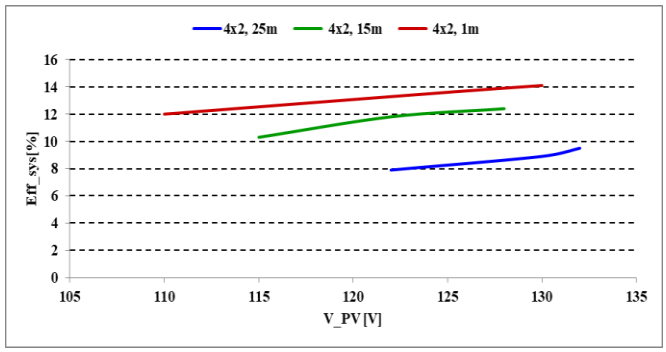

Figure 12. System efficiency for 4S2P configuration

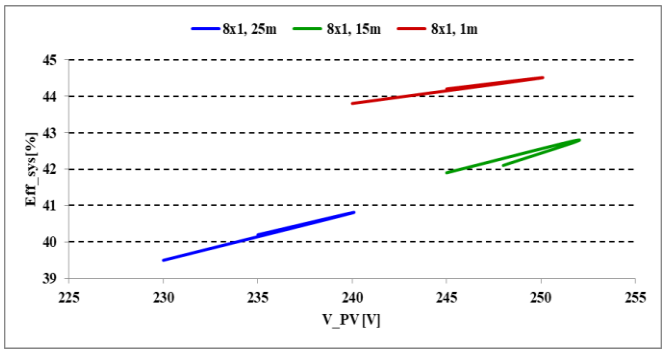

Figure 13. System efficiency for 8S1P configuration

When VPV falls below 200 V, the controller's built-in low-voltage protection activates. As stated in the Jntech controller manual (and confirmed by the provided specification sheet), the device is designed to handle under-voltage conditions without shutting down entirely. Instead, it transitions into a non-MPPT, protected operating mode to prevent damage to the pump motor. The system continues to deliver water, but at a drastically reduced efficiency because the operating point drifts far from the true MPP.

Thus, "MPPT failure" in the 4S2P case is not a complete shutdown but a transition to open-loop, non-optimized operation—a direct consequence of the controller's protective design, which prioritizes system safety over maximum power extraction under marginal voltage conditions.

Table 2 provides a quantitative comparison of the electrical and hydraulic performance of the 8S1P and 4S2P PV array configurations at three representative operating times (08:00, 12:00, and 16:00) under total heads of 1 m, 15 m, and 25 m. Across all conditions evaluated, the 8S1P configuration demonstrates superior performance in every major metric—PV voltage, current, power output, water flow rate, and overall system efficiency. These results reinforce the conclusion that array topology and resulting voltage level are the primary determinants of system productivity.

Table 2. Comparative table of system performance differences

Config.	Head [m]	Time [h]	V_{PV} [V]	I_{PV} [A]	P_{PV} [W]	Q [m^3/h]	Eff_sys [%]
8S1P	1	8	220	7.0	1540	7.0	40.2
		12	250	7.6	1900	9.0	44.5
		16	225	7.2	1620	7.5	41.5
	15	8	225	6.8	1530	7.5	40.8
		12	252	7.3	1839	9.0	42.8
		16	230	6.9	1587	7.8	40.5
	25	8	210	6.5	1365	6.5	39.0
		12	240	7.1	1704	8.0	40.8
		16	215	6.7	1441	6.8	38.5
4S2P	1	8	110	2.4	264	4.0	12.0
		12	130	2.9	377	5.5	14.1
		14	128	2.8	358	5.3	13.9
	15	8	115	2.5	288	2.2	10.3
		12	128	3.1	397	3.8	12.4
		14	125	3.0	375	3.6	12.2
	25	8	122	2.0	244	0.8	7.9
		12	132	2.3	304	1.3	9.5
		16	128	2.1	269	1.0	8.7

Specifically, the 8S1P configuration maintains operating voltages within the inverter's valid MPPT activation window, enabling the controller to draw high current (6.5–7.6 A) and consequently deliver elevated power levels (1365–1900 W). This effective electrical performance translates into high flow rates (6.5–9.0 $m^3 \cdot h^{-1}$) and efficiencies ranging from 38.5–44.5%, characteristic of a well-matched PV–pump system. In contrast, the 4S2P configuration consistently operates below the MPPT voltage threshold (110–132 V), forcing the controller into a fixed-duty, non-tracking mode. As a result, current (2.0–3.1 A), power (244–397 W), and flow rate (0.8–5.5 $m^3 \cdot h^{-1}$) are severely diminished, and system efficiency is restricted to only 7.9–14.1%. Overall, these quantitative data provide conclusive evidence that insufficient PV voltage in the 4S2P configuration causes systematic underperformance, independent of hydraulic head or irradiance conditions.

4. CONCLUSIONS

This study experimentally evaluated two PV array configurations, 8S1P and 4S2P, coupled to a BLDC motor-driven water pump under the extreme climatic conditions of Ghardaia, Algeria. Performance was assessed across a range of total dynamic heads (1 m, 15 m, and 25 m).

The results clearly demonstrate that the 8S×1P configuration significantly outperformed the 4S×2P arrangement across all tested conditions. Its higher string voltage ensured stable operation within the input voltage window of the MPPT controller, enabling consistent and efficient power extraction from the PV array. As a result, the 8S1P system delivered higher motor efficiency, greater electrical to hydraulic energy conversion, and substantially increased water flow rates.

In contrast, the 4S2P configuration operated below the MPPT controller's minimum voltage threshold throughout the day. This resulted in the feature not being activated the MPPT, significant energy losses, and markedly reduced water output, highlighting a crucial point in the design of PV generators.

These findings underscore a key design imperative: in BLDC-based solar water pumping systems, the PV array voltage must be deliberately aligned with the inverter and MPPT controller's operational voltage range—not merely matched to nominal power ratings. This alignment is especially crucial in high-head, high-efficiency, or low-irradiance applications where voltage margins directly dictate system availability and performance.

For optimal sizing of a photovoltaic pumping system, it is not enough to consider only the system's power demand. The inverter's input voltage also plays a crucial role in ensuring efficient configuration. This voltage must fall within the MPPT range specific to each inverter type to optimize system operation.

Beyond technical validation, this work reinforces the suitability of BLDC motor pumps for sustainable water access in arid and remote regions. More importantly, it offers actionable, field-tested guidance for engineers and practitioners on optimizing PV array architecture to maximize water productivity, energy efficiency, and long-term reliability in off-grid solar pumping deployments.

REFERENCES

[1] IEA. (2022). World Energy Outlook 2022. IEA, Paris. https://www.iea.org/reports/world-energy-outlook-2022.

[2] Tsafarakis, O., van Sark, W.G. (2023). A density-based

time-series data analysis methodology for shadow detection in rooftop photovoltaic systems. Progress in Photovoltaics: Research and Applications, 31(5): 506-523. https://doi.org/10.1002/pip.3654

[3] Luque, A., Hegedus, S. (2003). Handbook of Photovoltaic Science and Engineering. John Wiley & Sons.

[4] Zhou, J.H., Xu, M., Sun, J.L., Lee, F.C. (2005). A self-driven soft-switching voltage regulator for future microprocessors. IEEE Transactions on Power Electronics, 20(4): 806-814. https://doi.org/10.1109/TPEL.2005.850924

[5] Czanderna, A.W., Pern, F.J. (1996). Estimating service lifetimes of a polymer encapsulant for photovoltaic modules from accelerated testing. In Conference Record of the Twenty Fifth IEEE Photovoltaic Specialists Conference-1996, Washington, DC, USA, pp. 1219-1222. https://doi.org/10.1109/PVSC.1996.564351

[6] Benbaha, N., Zidani, F., Bouchakour, A., Boukebbous, S.E., Nait-Said, M.S., Ammar, H., Bouhoun, S. (2021). Optimal configuration investigation for photovoltaic water pumping system, case study: In a desert environment at Ghardaia, Algeria. Journal européen des systèmes automatisés, 54(4): 549-558. https://doi.org/10.18280/jesa.540404

[7] Boukebbous, S.E., Benbaha, N., Bouchakour, A., Ammar, H., Bouhoun, S., Kerdoun, D. (2022). Experimental performance assessment of photovoltaic water pumping system for agricultural irrigation in semi-arid environment of Sebseb—Ghardaia, Algeria. International Journal of Energy and Environmental Engineering, 13: 979-994. https://doi.org/10.1007/s40095-021-00435-8

[8] Ammar, H., Benbaha, N., Boukebbous, S.E. (2017). P&O control of a photovoltaic pumping system to efficiency improvement using PSIM. In 2017 International Renewable and Sustainable Energy Conference (IRSEC), Tangier, Morocco, pp. 1-5. https://doi.org/10.1109/IRSEC.2017.8477404

[9] Kumar, R., Singh, B. (2016). BLDC motor-driven solar PV array-fed water pumping system employing zeta converter. IEEE Transactions on Industry Applications, 52(3): 2315-2322. https://doi.org/10.1109/TIA.2016.2522943

[10] Balakumar, S., Lemma, M., Godato, M. (2025). Solar-powered ANN-based MPPT with zeta converter for BLDC motor water pumping in rural Ethiopia for sustainable agriculture. Discover Sustainability, 6: 140. https://doi.org/10.1007/s43621-025-00893-8

[11] Kumar, R., Singh, B. (2014). Solar photovoltaic array fed Luo converter based BLDC motor driven water pumping system. In 2014 9th International Conference on Industrial and Information Systems (ICIIS), Gwalior, India, pp. 1-5. https://doi.org/10.1109/ICIINFS.2014.7036591.

[12] Vikram, A.A., Navaneeth, R., Kumar, M.N., Vinoth, R. (2018). Solar PV array fed BLDC motor using zeta converter for water pumping applications. Journal of Science and Technology (JST), 3(4): 8-19. https://jst.org.in/index.php/pub/article/view/184.

[13] Khazaee, A., Zarchi, H.A., Markadeh, G.R.A. (2020). Real-time maximum torque per ampere control of brushless DC motor drive with minimum torque ripple. IEEE Transactions on Power Electronics, 35(2): 1194-1199. https://doi.org/10.1109/TPEL.2019.2918711

[14] Singh, D.B., Mahajan, A., Devli, D., Bharti, K., Kandari, S., Mittal, G. (2021). A mini review on solar energy based pumping system for irrigation. Materials Today: Proceedings, 43: 417-425. https://doi.org/10.1016/j.matpr.2020.11.716

[15] Prabhu, N., Thirumalaivasan, R., Ashok, B. (2023). Critical review on torque ripple sources and mitigation control strategies of BLDC motors in electric vehicle applications. IEEE Access, 11: 115699-115739. https://doi.org/10.1109/ACCESS.2023.3324419

[16] Antony, R.P., Komarasamy, P.R.G., Rajamanickam, N., Alroobaea, R., Aboelmagd, Y. (2024). Optimal rotor design and analysis of energy-efficient brushless dc motor-driven centrifugal monoset pump for agriculture applications. Energies, 17(10): 2280. https://doi.org/10.3390/en17102280

[17] Malla, J.M.R., Bassi, W., Salman, M.A., Mondal, K., Sharma, A., Kandi, B.P., Malla, S.G. (2025). Botox optimization algorithm for MPPT of SPV powered BLDC motor driven water pumping system using FOPID controllers. Engineering Research Express, 7(1): 015361. https://doi.org/10.1088/2631-8695/adb7b7

[18] Mozaffari Niapour, S.A.K., Danyali, S., Sharifian, M.B.B., Feyzi, M.R. (2011). Brushless DC motor drives supplied by PV power system based on Z-source inverter and FL-IC MPPT controller. Energy Conversion and Management, 52(8-9): 3043-3059. https://doi.org/10.1016/j.enconman.2011.04.016

[19] Radhika, G., Kumar, D.R., Upadhyay, P., Ketan, C.A. (2024, July). Optimizing solar power extraction in water pumping: A comparison of fuzzy logic and inc mppt control. In 2024 IEEE 4th International Conference on Sustainable Energy and Future Electric Transportation (SEFET), Hyderabad, India, pp. 01-06. https://doi.org/10.1109/SEFET61574.2024.10718230

[20] Kumar, D., Tabrez, M., Choudhary, S.D., Mahmood, F.M. (2024). BLDC motor driven water pumping system powered by solar photovoltaics (PV). In Photovoltaic Systems Technology, pp. 211-224. https://doi.org/10.1002/9781394167678.ch11

[21] Kumar, P., Bhaskar, D.V., Behera, R.K., Muduli, U.R. (2023). Continuous fast terminal sliding surface-based sensorless speed control of PMBLDCM drive. IEEE Transactions on Industrial Electronics, 70(10): 9786-9798. https://doi.org/10.1109/TIE.2022.3225850

[22] Li, Z.C., Fan, X.W., Kong, Q.Y., Liu, J., Zhang, S. (2024). Torque ripple suppression of BLDCM with optimal duty cycle and switch state by FCS-MPC. IEEE Open Journal of Power Electronics, 5: 381-391. https://doi.org/10.1109/OJPEL.2024.3368221

[23] Prakash, A., Naveen, C. (2023). Combined strategy for tuning sensor-less brushless DC motor using SEPIC converter to reduce torque ripple. ISA Transactions, 133: 328-344. https://doi.org/10.1016/j.isatra.2022.06.045

[24] Tadivalasa, V., Biswas, P.K., Das, U., Thanikanti, S.B., Selvarajan, S. (2025). Optimized PV fed sensorless BLDC motor control system using Q-recurrent adaptive controller and Levy-enhanced circular search mechanisms. Scientific Reports, 15: 42701. https://doi.org/10.1038/s41598-025-26884-3

[25] Benbaha, N., Zidani, F., Nait-Said, M.S., Zouzou, S.E., Boukebbous, S., Ammar, H. (2018). dSPACE validation of improved backstepping optimal energy control for

photovoltaic systems. In 2018 6th International Renewable and Sustainable Energy Conference (IRSEC), Rabat, Morocco, pp. 1-6. https://doi.org/10.1109/IRSEC.2018.8702908
[26] Sadrossadat, S.A., Rahmani, O. (2020). ANN-based method for parametric modelling and optimising efficiency, output power and material cost of BLDC motor. IET Electric Power Applications, 14(6): 951-960. https://doi.org/10.1049/iet-epa.2019.0686
[27] Tripathy, S.N., Kundu, S., Pradhan, A., Samal, P. (2024). Optimal design of a BLDC motor using African vulture optimization algorithm. e-Prime-Advances in Electrical Engineering, Electronics and Energy, 7: 100499. https://doi.org/10.1016/j.prime.2024.100499
[28] Chakkarapani, K., Thangavelu, T., Dharmalingam, K., Thandavarayan, P. (2019). Multiobjective design optimization and analysis of magnetic flux distribution for slotless permanent magnet brushless DC motor using evolutionary algorithms. Journal of Magnetism and Magnetic Materials, 476: 524-537. https://doi.org/10.1016/j.jmmm.2019.01.029

NOMENCLATURE

I	Output current of the PV module
V	Output voltage of the PV module
Tc	PV cell temperature (°C)
G	Solar irradiance (W/m²)
Pmax	Maximum power output
Vmp	Voltage at maximum power point
Imp	Current at maximum power point
Voc	Open-circuit voltage
Isc	Short-circuit current
η	System or component efficiency
D	Duty cycle of the DC–DC converter
VDC	DC-link voltage
Fsw	Switching frequency
PV	Photovoltaic
SPV	Solar Photovoltaic
BLDC	Brushless DC motor
MPPT	Maximum Power Point Tracking
STC	Standard Test Conditions (1000 W/m², 25°C, AM1.5)
DC	Direct Current
AC	Alternating Current
P&O	Perturb and Observe (MPPT algorithm)
FOC	Field-Oriented Control
MPP	Maximum Power Point
I–V	Current–Voltage
P–V	Power–Voltage
DC–DC	Direct Current to Direct Current converter
max	Subscript: at maximum power point
oc	Subscript: open-circuit condition
sc	Subscript: short-circuit condition
ref	Subscript: reference value (e.g., at STC)
in	Subscript: input
out	Subscript: output

APPENDIX

Table A1. AC/DC solar pump controller specifications

Model	JNPH200
Adaptable Pump	Rated 200 V pump
Rated Input Power (kW)	1.8
Max. Input Current (A)	17.0
Max. Input Voltage (V)	DC420 V / AC280 V
Min. Input Voltage (V)	DC80 V / AC85 V
Optional MPPT Voltage (V)	200 ~ 400
Working Environment (°C)	-15 ~ 60

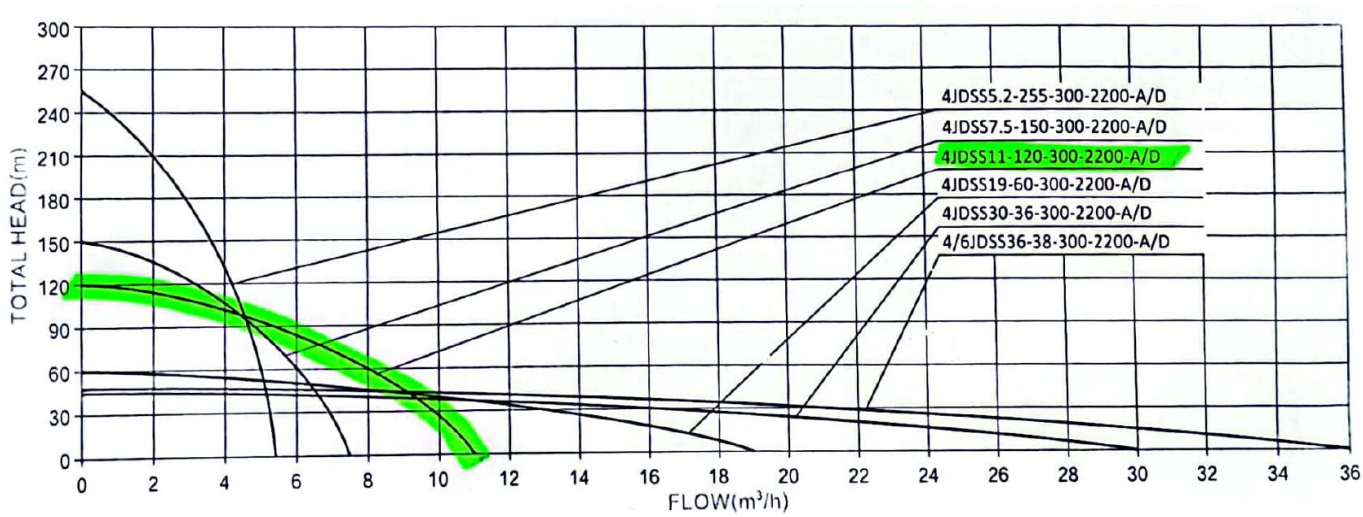

Figure A1. Jntech solar pump hydraulic performance curves